Application of self-tuning Gaussian networks for control of civil structures equipped with magnetorheological dampers

Citation: Laflamme, Simon, and Jerome J. Connor. "Application of self-tuning Gaussian networks for control of civil structures equipped with magnetorheological dampers." Active and Passive Smart Structures and Integrated Systems 2009. Ed. Mehdi Ahmadian & Mehrdad N. Ghasemi-Nejhad. San Diego, CA, USA: SPIE, 2009. 72880M-12. © 2009 SPIE

As Published: http://dx.doi.org/10.1117/12.815540

Publisher: Society of Photo-Optical Instrumentation Engineers

Persistent URL: http://hdl.handle.net/1721.1/52638

Version: Final published version: final published article, as it appeared in a journal, conference proceedings, or other formally published context

Application of self-tuning Gaussian networks for control of civil structures equipped with magnetorheological dampers

Simon Laflamme* and Jerome J. Connor
Dept. of Civil and Env. Eng., MIT, 77 Mass. av., Cambridge, MA 02139

ABSTRACT

This paper proposes an adaptive neural network composed of Gaussian radial functions for mapping the behavior of civil structures controlled with magnetorheological dampers. The online adaptation takes into account the limited force output of the semi-active dampers using a sliding mode controller, as their reaction forces are state dependent. The structural response and the actual forces from the dampers are used to adapt the Gaussian network by tuning the radial function widths, centers, and weights. In order to accelerate convergence of the Gaussian radial function network during extraordinary external excitations, the learning rates are also adaptive. The proposed controller is simulated using three types of earthquakes: near-field, mid-field, and far-field. Results show that the neural controller is effective for controlling a structure equipped with a magnetorheological damper, as it achieves a performance similar to the passive-on strategy while requiring as low as half the voltage input.

Keywords: Gaussian radial functions, magnetorheological dampers, adaptive control, structural control, civil structures

1. INTRODUCTION

Specific problems associated with variable control of civil structures include large actuating forces, possible destabilization from feedback control, uncertainties in dynamic characteristics, and limited state measurements[1]. Magnetorheological (MR) dampers have been proposed in the literature for control of civil structures because of their capability to perform almost as well as active control schemes, while requiring only a fraction of the power input[2,3].They are also considered to be robust and fail-safe[4], providing enhanced protection for vibration mitigation during natural hazards. Their hysteretic behavior has been extensively studied and successfully modeled[5], but their complex dynamic behavior renders complicated the mapping of the required voltage for a desired force[6]. Even when such mapping is possible, knowledge of the dynamic properties of the structure is required. However, dynamic characteristics of structures are inherently difficult to estimate accurately. Some control techniques have been proposed to account for bounded uncertainties, such as sliding mode control[7] and adapted LQR/H_2 control[8], but a nominal estimation of the plant characteristics is still required as the performance of the controller depends on the level of the uncertainties. Neural nets have been proposed to deal with uncertainties without prior knowledge of the plant, attempting to map the entire plant/MR damper system[9,10]. However, classic neural networks must be trained a priori, which is difficult to achieve for large-scale structures. Suresh *et al.*[11] proposed an adaptive mapping scheme based on Lyapunov stability theory that uses Gaussian radial functions to control base-isolation of nonlinear buildings equipped with an actuator. With the proposed mapping, the structure learns its behavior during an event while using limited state measurements. Lee *et al.*[12] developed a semi active neuro-controller for base-isolation control with an MR damper, where the neural network was updated using a cost function and sensitivity evaluation. Lee *et al.*[13] achieved an adaptive modal neuro-controller for a structure equipped with a MR damper. Song *et al.*[14] proposed an adaptive controller for MR dampers used in car suspension systems. The controlled system is identified sequentially, and also includes an adaptive controller in parallel. System identification is achieved on a single degree-of-freedom system using a root least square algorithm, but such identification strategy would require too much computation time for a real-time application to civil structures because of the numerous degrees-of-freedom.

The main contribution of this paper is to propose a modified version of the self-tuning Gaussian network from Suresh *et al.*[11] to map the behavior of a civil structure equipped with MR dampers. Semi-active damping devices offer a

* laflamme@mit.edu; phone 1-617-452-3063

Active and Passive Smart Structures and Integrated Systems 2009, edited by Mehdi Ahmadian, Mehrdad N. Ghasemi-Nejhad, Proc. of SPIE Vol. 7288, 72880M · © 2009 SPIE · CCC code: 0277-786X/09/$18 · doi: 10.1117/12.815540

particular challenge in adaptive control since the state dependence of their reaction force means the desired control force may not be achieved. Therefore, the sequential training must take into account the uncertainty in the applied force. A sliding mode controller is used for this task. Moreover, the proposed self-tuning network uses adaptive learning rates based on Lyapunov stability theory to accelerate convergence. Many control schemes have been proposed in the structural control field since its introduction by Yao in 1972, but their applicability has not been extensively discussed[15]. This paper is also original as it discusses the applicability of the control solution to large-scale civil structures.

The paper is organized as follows: section 2 presents MR damper theory; section 3 reviews the GRF network design procedure; section 4 describes the proposed controller; section 5 contains the simulation and results along with a discussion; section 6 concludes the paper.

2. MAGNETORHEOLOGICAL DAMPERS

Magnetorheological actuators are defined by the fluid that gives them their rheological properties. This particular fluid contains polarizable and magnetizable particles that line up upon magnetic excitation, causing a change in the liquid's viscosity within a few milliseconds[16]. For a large-scale 180 kN MR damper, this response would be on the order of 60 milliseconds[17].

Their low power requirement, which is 50 W for a 200 kN damping force[5], also makes them very attractive as only a battery is needed to drive their response. This would allow the structure to remain stable under a global power failure which is likely to occur during a natural disaster, and in the event of a local power failure, MR dampers can still act as passive dampers, providing a minimal damping to the structure.

Numerous models, mathematical as well as non-mathematical, have been developed over the years in attempts to model the dynamic behavior of the damper. Spencer *et al*.[3] proposed a phenomenological model that has been shown to be quite accurate. This model is used for the computer simulation. According to this phenomenological model, the force output of an MR damper due to an applied voltage can be written as:

$$\begin{aligned} f &= c_1\dot{y} + k_1(x - x_0) \\ \dot{z} &= -\gamma|\dot{x} - \dot{y}|z|z|^{n-1} - \beta(\dot{x} - \dot{y})|z|^n + A(\dot{x} - \dot{y}) \\ \dot{y} &= (c_0 + c_1)^{-1}\left(az + c_0\dot{x} + k_0(x - y)\right) \end{aligned} \tag{1}$$

where f is the resulting force, $k_0, k_1, \beta, \gamma, A, n$ are constants, z is an evolutionary variable, and $a, c_0, c_1$are voltage-dependent and defined by:

$$\begin{aligned} a &= a_a + a_b w \\ c_0 &= c_{0a} + c_{0b} w \\ c_1 &= c_{1a} + c_{1b} w \\ \dot{w} &= -\eta(w - v) \end{aligned} \tag{2}$$

where $a_a, a_b, c_{0a}, c_{0b}, c_{1a}, c_{1b}, \eta$ are constants, v is the applied voltage, and *w* is the actual voltage.

The inverse mapping of voltage to force is difficult to achieve with most mathematical models, as seen from equations (1) and (2). It is possible to use a neural network to identify this inverse mapping, but this necessitates prior training. Since this paper is an effort to propose a system that could work without prior training, the required force from the controller is applied following the clipped-optimal algorithm[18]. In this algorithm, the applied voltage is maximum if the required force is higher than the actual damper force and of the same sign; it is set to zero otherwise. The clipped-optimal algorithm has shown good performance in the literature[2,19]. It can be directly observed from the clipped-optimal scheme that there will be an error between the actual force u_{act} and the required force u:

$$\tilde{u} = u - u_{act} \tag{3}$$

This error $\tilde{u}$ on the force is treated as a system uncertainty and is handled using a sliding mode controller described in section 4.

3. GAUSSIAN NETWORKS

Neural networks have attracted significant attention over the past decades because of their capability to approximate the input-output relationship of unknown systems. Traditionally, sigmoid and linear functions are combined linearly to achieve the system approximation. More recently, Gaussian radial functions (GRF) have been researched to replace traditional functions[20]. GRF neural network have several advantages compared to traditional neural nets, among which are better approximation, convergence speed, optimality in solution and excellent localization[11]. The choice of Gaussian radial functions (GRF) is also motivated by their capability to be trained more quickly than most other neural network techniques, and to model nonlinear systems by estimating in the function space[20-22]. The output of a GRF network can be expressed as:

$$\Theta_{\mathrm{j}} = \sum_{k=1}^{h} \alpha_{kj} e^{-\frac{\|X-\mu_k\|^2}{\sigma_k^2}} = \alpha_j^T \phi, \qquad j = 1, 2, 3, \ldots m \tag{4}$$

where Θ is the output, X is the input vector; the α and σ are vectors containing the network weights and the Gaussian widths; μ is a matrix containing the multidimensional location of the Gaussian centers; ϕ is the vector representing Gaussian functions; and subscripts j and k range over the number of output and Gaussian functions, respectively.

3.3.1 Network Input/Output

The GRF network designed for this paper is a direct inverse controller, where the artificial neural network outputs control forces according to some states. The choice of the number of outputs is straightforward, and corresponds to the number of actuators. The choice of state input, however, is more involved, and needs to be selected based on prior knowledge of the system, if possible. The network designer must also choose an appropriate lag space, which has to be large enough to include the dynamics that properly describes the system, and decide on an appropriate scaling of input which would improve the algorithm robustness and convergence speed[23].

3.3.2 Self-Organization of Nodes

GRF network performance depends on the number of basis functions and on the width and position of the center of each function. Generally, the network has to be a priori trained with an existing set of input-output. However, this is difficult to achieve for civil structures because of the size of the structures to be controlled. Therefore, sequential learning is preferred over batch learning. The concept of sequential learning is that the neural network learns, or adapts, after each new input-output entry. Nevertheless, because of the lack of prior information on the set of input-output data, pre-set numbers of tuned GRF result in suboptimal networks[24]. A self-organizing neural network model (SOM) has the capability to adapt itself, by adding or subtracting nodes, which motivates the choice of a self-organizing GRF network for this paper.

Based on SOM theory, nodes are added when a new set of input is too far from the actual node centers. The new node is generally placed at the center of the new set, with appropriate weight to achieve the output, and of a pre-defined width. A SOM can also have the capability to prune nodes when they are judged to be unnecessary. Many different rules can be set to prune a network. For instance, one can choose to remove a node if its weight falls below a threshold for a certain continuous number of observations.

3.3.3 Adaptation of Parameters

There exist many algorithms to adapt network parameters, such as back-propagation (BP), extended Kalman filtering, and recursive least-square, but the BP algorithms is clearly superior in its computational simplicity[25]. Applicability of the neural controller for real-time control requires computational simplicity and minimal data storage in order to avoid time

delay. The BP scheme has slow convergence. However, convergence is improved by including learning parameters that estimates the size of the step to be taken in the direction of the steepest descent. It is difficult to choose appropriate learning parameters in the case of a structure exposed to stochastic excitations because of the unknown magnitude of the dynamic response. Behera *et al.*[25] proposed time-varying learning parameters that enhance convergence speed for system identification, and showed their stability via Lyapunov theory. The concept of time-varying learning rates is implemented in the proposed neural controller.

4. CONTROLLER

Based on (4), the mapping of control-input/state-output of the system equipped with a MR damper can be expressed as:

$$u_{d,j} = \alpha_j^T \phi, \qquad j = 1, 2, 3, \ldots m \tag{5}$$

where u_d is the desired control force. Because the proposed controller will be applied to a single actuator, this section is specialized for the case where $j = 1$.

Using (5) and the conventional state-space representation of the equation of motion of a structure, the dynamics of the controlled state error can be written as:

$$\begin{aligned} \dot{e} = \dot{x} - \dot{x}_d &= Ae + B(u_{act} - u_d + \epsilon) \\ &= Ae + B\left(\hat{\alpha}^T\hat{\phi} - \alpha^T\phi - \tilde{u} + \epsilon\right) \end{aligned} \tag{6}$$

where x is the system state vector, A, B, and u are notations that conform to the traditional state-space representation of dynamic systems, the subscript d denotes the desired states and forces (optimal), the hat denotes estimated values, and ϵ is the estimation error. Using a sliding mode controller and defining the sliding surface as:

$$s = Pe \tag{7}$$

where the targeted surface is $s = 0$, P is a user-defined vector with all positive elements weighting the error vector, and introducing the following control law:

$$u_{act} = \hat{\alpha}^T\hat{\phi} - k\big(\text{sign}(s)\big) \tag{8}$$

where k is a constant to be defined later, (6) becomes:

$$\dot{e} = Ae + B\left(\hat{\alpha}^T\hat{\phi} - \alpha^T\phi - \tilde{u} + \epsilon - k\big(\text{sign}(s)\big)\right) \tag{9}$$

Note that (8) uses a sign function rather than a saturation function. Even though a saturation function would help a smoother transition in the control force, thus preventing chattering, using the clipped-optimal algorithm transforms this control law into a bang-bang controller on the voltage input.

In order to find adaptation laws that would guarantee the stability of the GRF network, Lyapunov theory is applied. Consider the following Lyapunov candidate:

$$V = \frac{1}{2}\left[s^T s + \tilde{\alpha}^T\Gamma_\alpha^{-1}\tilde{\alpha} + \tilde{\phi}^T\Gamma_\phi^{-1}\tilde{\phi}\right] \tag{10}$$

where Γ_α^{-1} and Γ_ϕ^{-1} are positive definite diagonal matrices representing learning parameters, the tilde denotes the error between the estimated and real values ($\tilde{\alpha} = \hat{\alpha} - \alpha; \tilde{\phi} = \hat{\phi} - \phi$). Note that here s is a scalar, but because it becomes a column vector in the case of multiple MR dampers, it is written in vector form. Neglecting the higher order term, the time derivative of V is:

$$\begin{aligned}\dot{V} &= s^T PAe + s^T PB\left(\hat{\alpha}^T\tilde{\phi} + \tilde{\alpha}^T\hat{\phi}\right) + \tilde{\alpha}^T\Gamma_\alpha^{-1}\dot{\hat{\alpha}} + \tilde{\phi}^T\Gamma_\phi^{-1}\dot{\hat{\phi}} + \tilde{\alpha}^T\dot{\Gamma}_\alpha^{-1}\tilde{\alpha} + \tilde{\phi}^T\dot{\Gamma}_\phi^{-1}\tilde{\phi} + s^T PB\epsilon \\ &\quad - s^T PB\tilde{u} - |s^T|PBk \\ &= e^T P^T PAe + \tilde{\phi}^T\left(\hat{\alpha}^T B^T P^T s + \Gamma_\phi^{-1}\dot{\hat{\phi}}\right) + \tilde{\alpha}^T\left(\hat{\phi}^T B^T P^T s + \Gamma_\alpha^{-1}\dot{\hat{\alpha}}\right) - s^T PB(\tilde{u} - \epsilon) - |s^T|PBk \\ &\quad + \tilde{\xi}^T\dot{\Gamma}^{-1}\tilde{\xi}\end{aligned} \tag{11}$$

with:

$$\tilde{\xi} = \begin{bmatrix}\tilde{\alpha} \\ \tilde{\phi}\end{bmatrix}, \Gamma = \begin{bmatrix}\Gamma_\alpha & 0 \\ 0 & \Gamma_\phi\end{bmatrix}$$

The tilde denotes the error between the optimal and current parameters. By choosing the following adaptation laws:

$$\begin{aligned}\dot{\hat{\alpha}} &= -\left(\Gamma_\alpha\hat{\phi}\right)B^T P^T s \\ \dot{\hat{\phi}} &= -\left(\Gamma_\phi\hat{\alpha}\right)B^T P^T s \\ \dot{\Gamma}^{-1} &= -s^T sI\end{aligned} \tag{12}$$

where I is an identity matrix to populate $\dot{\Gamma}^{-1}$, equation (11) becomes:

$$\dot{V} = e^T P^T PAe - s^T PB(\tilde{u} - \epsilon) - |s^T|PBk - \tilde{\xi}^T(s^T sI)\tilde{\xi} \tag{13}$$

Choosing $k = \eta u_b$, where η is positive, and u_b is a known bound (also positive) on $\tilde{u}$, (13) can be rewritten as:

$$\dot{V} = e^T P^T PAe - s^T PB(\tilde{u} - \epsilon) - |s^T|PB\eta u_b - \tilde{\xi}^T(s^T sI)\tilde{\xi} \tag{14}$$

It can be noted that the switching law in (8), and thus the term k, can be used to control for system uncertainties. The adaptive parameters are chosen to guarantee convergence of the GRF network based on the error. Hence, uncertainties on external loadings from both the desired and current dynamics are cancelled out in (6). The term k depends on the uncertainty on the error on the applied force u_b and a constant. This error can be quite large, and increasing its value too much would lead to a controller based almost exclusively on the sign of the sliding surface. Instead, a bound u_b is assumed, and adaptation on the network slowed when $|\tilde{u}| > u_b$.

The estimation error term ϵ is decreased with the increased number of GRF nodes. It is assumed that $\tilde{u}$ is much larger than ϵ, otherwise the switching control term will by default be larger than $\tilde{u} - \epsilon$. Therefore, equation (14) can be guaranteed to be negative for P chosen such that $P^T PA$ is semi-negative definite. Note that in practice the matrix A is unknown. Nevertheless, it is acceptable to choose P based on a rough approximation of A because of its structure and magnitude. Equation (14) is therefore negative definite. Thus, using *Barbalat's lemma*, the error will converge to zero[26].

4.1 Discussion on System States

The sliding surface necessitates the knowledge of all displacements and velocities, as well as for some of the input states in (4). To obtain these states, it is better to have an estimator. In practice, only accelerations are measured because displacement and velocity measurements only provide relative quantities, are more expensive to measure than accelerations, and integration of acceleration can lead to significant errors[27,28].

It is also worth mentioning that in the case where displacement and velocity measurements of some specific degrees of freedom cannot be obtained, the vector P can be modified to include null entries where these measurements are missing.

For the proposed controller, the input states are the actual displacements and velocities, and the previous applied forces. Despite that they have to be estimated in practice, using displacements and velocities is advantageous as these measures represent the error. This error is therefore fed in the neural network as an input. The velocity inputs are scaled by 10 and the forces by 1000 to give an equal importance in the network.

4.2 Self-Organization Rules

Conformed to the previous section, a node is added if the smallest distance between the center of an input and an existing node falls below a threshold. This threshold has to be selected depending on the type of excitation. For instance, this threshold will be higher if the region where the structure is located is expected to have earthquakes of large intensity. Regarding pruning, a node is removed if its weight falls below 5% of the highest weight for more than 100 consecutive samples.

4.3 Adaptive Learning Parameters

Noting that $\Gamma\Gamma^{-1} = I$, taking its time derivative results in:

$$\dot{\Gamma} = \Gamma(s^T s I)\Gamma \tag{15}$$

It is clear from (11) and (15) that the adaptive learning rate can be any increasing function, because $\dot{\Gamma}^{-1}$ has to be semi negative definite. Using the sliding surface error in the function is intuitive, as a greater error indicates that the system is further from its optimality, therefore increasing the step taken in the descent direction. However, in order to prevent the learning rate from augmenting too quickly, and thus initiating system instability, (15) is modified by dividing by the 2-norm of the learning rate. Therefore, noting that in the following equation Γ_ξ is the ξ^{th} diagonal parameter of the matrix Γ and thus a scalar, the adaptation laws (12) for the ξ^{th} network parameter can be rewritten as:

$$\begin{aligned} \dot{\hat{\xi}} &= -\Gamma_\xi \left(\frac{\delta u}{\delta \xi}\right) B^T P^T s \\ \dot{\Gamma_\xi} &= \mathrm{s^T s} \end{aligned} \tag{16}$$

While $\hat{\xi}$ is modified using an unknown vector B, it is noted that this adaptation can be realized using the approximation $\hat{B}$, as $\hat{B} = \psi B$ where ψ is a diagonal matrix, and that ψ can be absorbed in Γ.

5. SIMULATION

The three degree-of-freedom model tested in Dyke *et al.*[18] has been used as a benchmark for the numerical simulation. Just as with the benchmark model, a 1000 N MR damper is attached between the ground and the first story. Structural properties are as follows:

$$M = \begin{bmatrix} 98.3 & 0 & 0 \\ 0 & 98.3 & 0 \\ 0 & 0 & 98.3 \end{bmatrix} \mathrm{kg}; \quad C = \begin{bmatrix} 175 & -50 & 0 \\ -50 & 100 & -50 \\ 0 & -50 & 50 \end{bmatrix} \frac{\mathrm{N \cdot s}}{\mathrm{m}}; \quad K = 10^5 \begin{bmatrix} 12.0 & -6.84 & 0 \\ -6.84 & 13.7 & -6.84 \\ 0 & -6.84 & 6.84 \end{bmatrix} \frac{\mathrm{N}}{\mathrm{m}}$$

Three different earthquakes corresponding to far-field, mid-field, and near-field earthquakes are considered. The earthquakes are ElCentro 1940 North-South (near-field), Kobe 1995 East-West (mid-field), and Mexico City 1985 North-South (far-field). The earthquake time is scaled by a factor of 5 to match the model.

In order to show stability of the controller, the structure has been simulated with an ideal actuator saturating at 1100 N. The switching term has been used to account for a possible difference between the force predicted by the network and the actual force resulting from the actuator saturation. Figure 1 shows the neural controller performance at reducing the third story displacement for the ElCentro earthquake. Figure 2 shows the performance for a sinusoidal excitation at the first natural frequency.

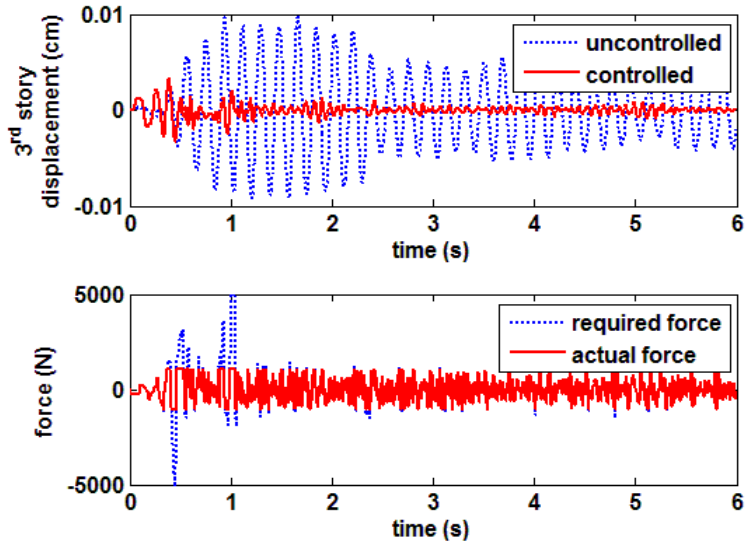

Figure 1: Controller performance, ElCentro earthquake.

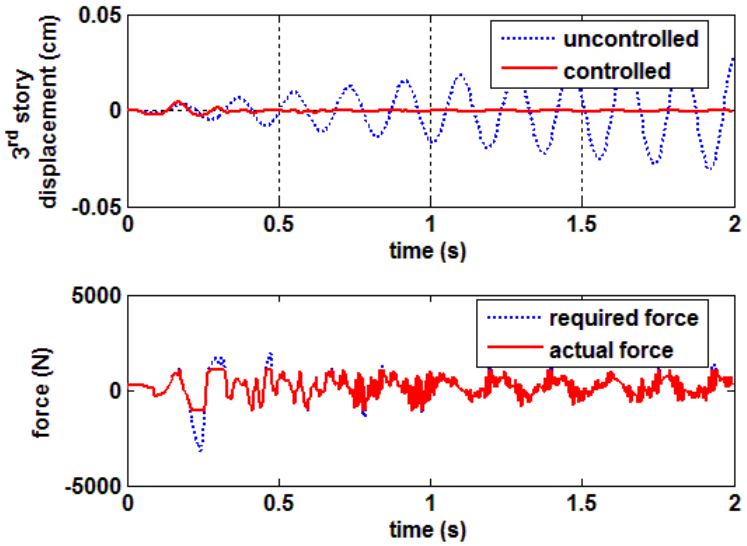

Figure 2: Controller performance, sinusoidal excitatio

The controller has been applied with the MR damper. Detailed performance for the ElCentro (1940) earthquake is shown in Figures 3 – 8. Figure 3 and Figure 4 show results for the third storey displacement and acceleration reduction. Figure 5 and Figure 6 compare vibration mitigation against the passive-off and passive-on case. The passive-off case refers to the utilization of the MR damper with no voltage input, while the passive-on case refers to the continuous application of the full voltage. Figure 7 shows the force from the MR damper, and Figure 8 compares the required force versus the actual force.

The controller has been tested against three different types of earthquakes. The evolutions of the GRF networks for the three earthquakes are plotted along with the excitations in Figures 5.9 – 5.11. Results are shown in Tables 1 – 3.

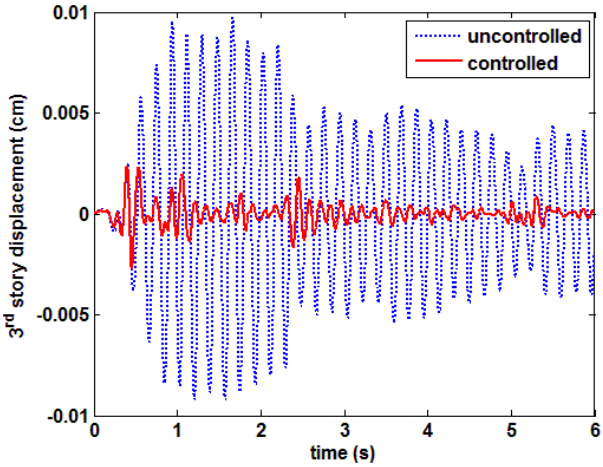

Figure 3: Third story displacement; uncontrolled versus controlled case.

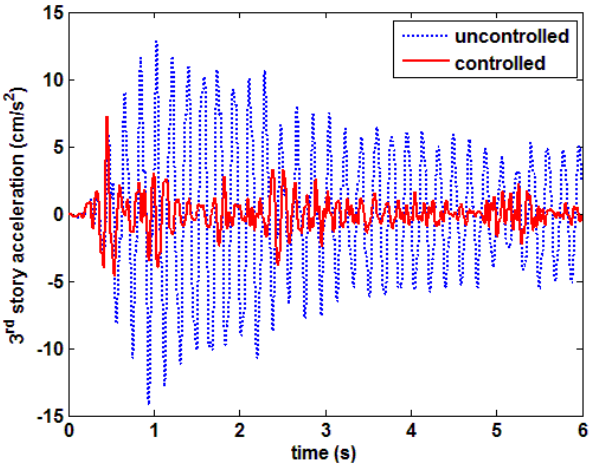

Figure 4: Third story acceleration; uncontrolled versus controlled case.

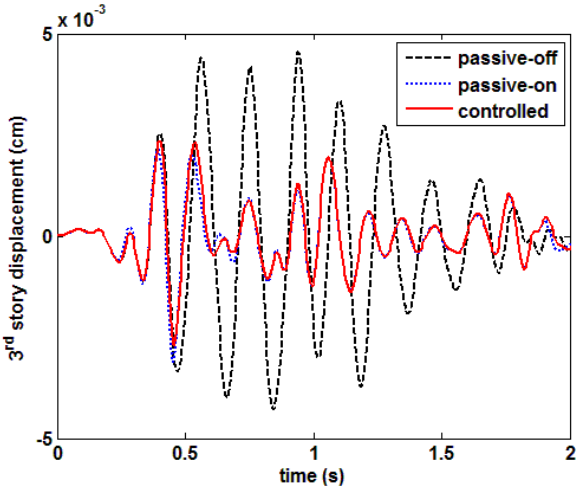

Figure 5: Third story displacement; passive versus controlled case.

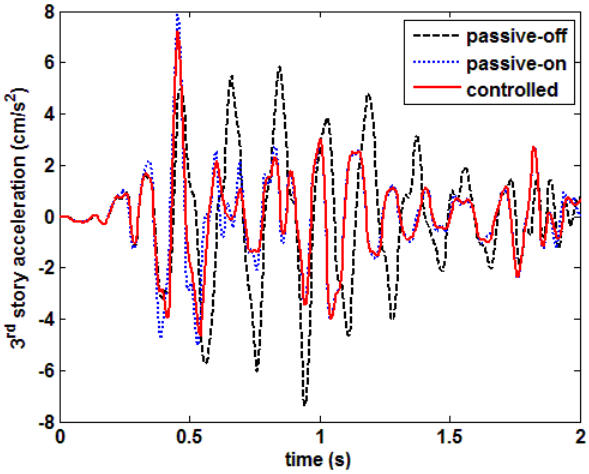

Figure 6: Third story acceleration; passive versus controlled case.

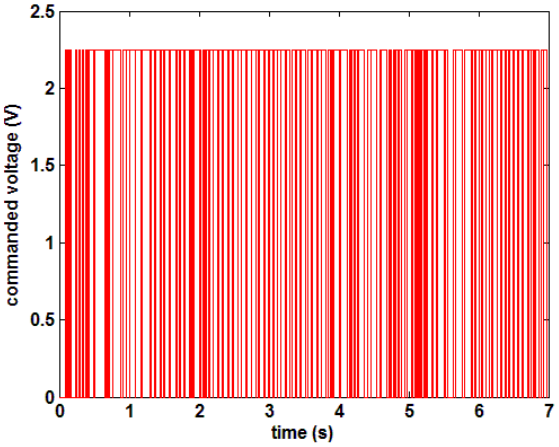

Figure 7: Applied voltage.

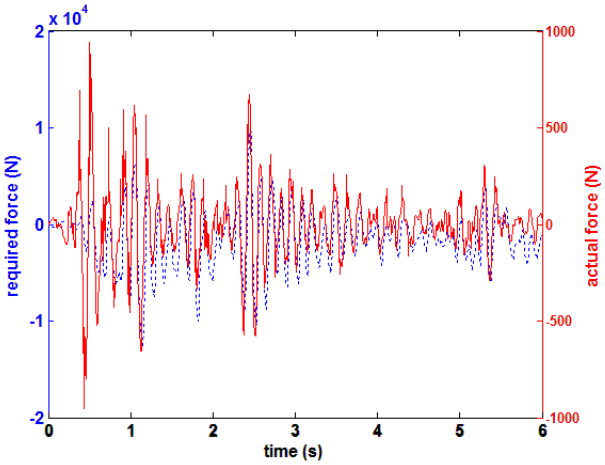

Figure 8: Required force (dotted line) versus actual force.

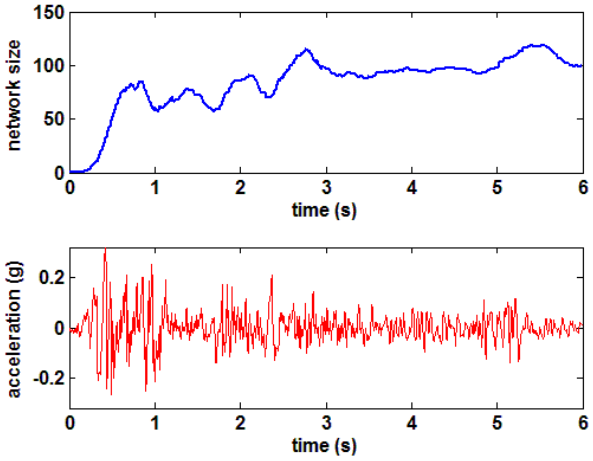

Figure 9: Evolution of the GRF network, ElCentro earthquake.

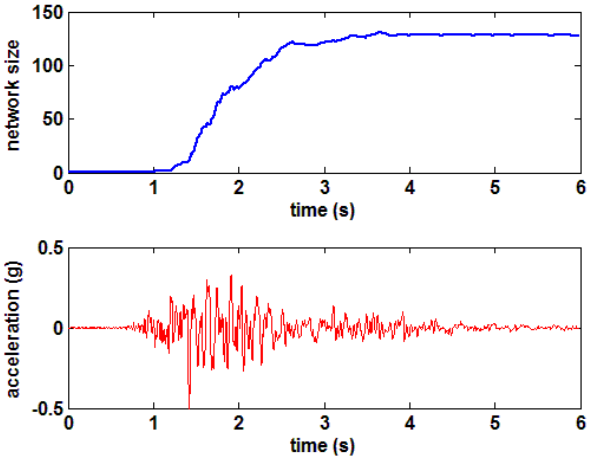

Figure 10: Evolution of the GRF network, Kobe earthquake.

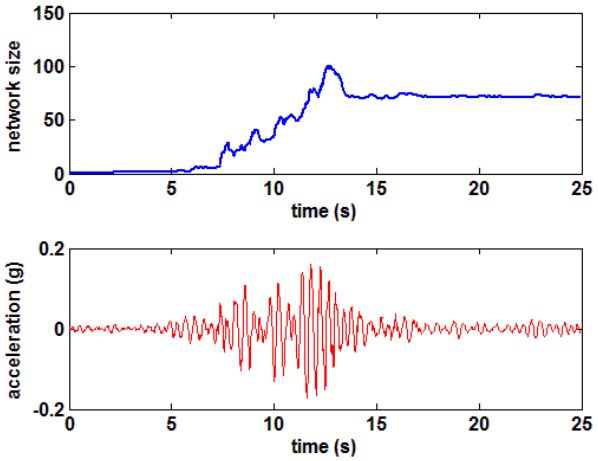

Figure 11: Evolution of the GRF network, Mexico City earthquake.

Near-Field - ElCentro 1940 NS

		Uncontrolled	Passive-off	Passive-on	Controlled
Displ. (cm)	Storey 1	0.55	0.212	0.0790	0.0865
	Storey 2	0.837	0.362	0.198	0.189
	Storey 3	0.974	0.457	0.312	0.270
Acc. (cm/s^2)	Storey 1	883	402	293	652
	Storey 2	1067	509	525	455
	Storey 3	1414	738	790	722
Average force (N)		0	83.1	128	125
Average voltage (V)		0	0	2.25	1.54
Maximum Force (N)		0	264	1006	951

Table 1: Results for the ElCentro earthquake.

Mid-Field - Kobe 1995 EW

		Uncontrolled	Passive-off	Passive-on	Controlled
Displ. (cm)	Storey 1	0.303	0.169	0.0735	0.0790
	Storey 2	0.493	0.291	0.201	0.203
	Storey 3	0.607	0.352	0.305	0.310
Acc. (cm/s^2)	Storey 1	610	297	427	512
	Storey 2	697	475	560	559
	Storey 3	901	538	741	763
Average force (N)		0	59.9	131	129
Average voltage (V)		0	0	2.25	1.29
Maximum Force (N)		0	223	1031	1075

Table 2: Results for Kobe earthquake.

Far-Field - Mexico City 1985 NS

		Uncontrolled	Passive-off	Passive-on	Controlled
Displ. (cm)	Storey 1	0.188	0.117	0.0810	0.0811
	Storey 2	0.291	0.189	0.129	0.131
	Storey 3	0.347	0.225	0.163	0.165
Acc. (cm/s^2)	Storey 1	274	226	170	530
	Storey 2	337	239	189	260
	Storey 3	391	285	245	289
Average force (N)		0	32.6	45.8	43.6
Average voltage (V)		0	0	2.25	1.07
Maximum Force (N)		0	156	472	649

Table 3: Results for Mexico City earthquake.

5.1 Discussion on Results

Results on the three earthquakes show that the controller is promising for vibration mitigation. With respect to displacement control, the controller mitigates vibrations similar to the passive-on case, but with significantly less voltage. Acceleration mitigation is better for the near-field earthquake, similar for the mid-field, and worst for the far-field, except for the first floor where the actuator is located. This increase in acceleration on the first floor is explained by the change in the damper voltage provoking a non-smooth displacement of the damper itself, as expected. However, the GRF network does not have acceleration mitigation as a goal, since it does not appear in the error metric.

The evolution of the networks show that the neural controller initially quickly increases in size when the earthquake occurs, and then stabilizes at the same time as the excitation, as evidenced with the Kobe and Mexico City earthquakes. This concept is quite intuitive, but shows that a rapid convergence of the network is essential to effectively achieve hazard mitigation.

Figure 8 depicts the major challenge faced when using adaptive control with an MR damper. The semi-active control device can only work towards achieving the required force, but usually does not achieve it. This results in a slow convergence of the neural network, which necessitates taking bigger steps in the descent direction. Nevertheless, no structural instability can occur because of the inherent stability of damping devices. This comparison in forces shows that the force outputted by the damper successfully follows a scaled version of the force required by the neural controller.

6. CONCLUSION

Results show that the use of a GRF neural network to control an MR damper is promising. The damper was capable of significantly mitigating vibrations with a fraction of the voltage required to do so with a passive-on strategy. This performance is similar for all three types of simulated earthquakes.

More work has to be done in order to optimize the choice of parameters used in the network design, such as for the self-organization rules. Other performance measures could be tested with the controller, such as acceleration reduction. A neuro-controller based on pure acceleration feedback is currently being researched by the authors.

The proposed control strategy is particularly attractive for large-scale implementation. It does not require prior knowledge of structural properties, as parameters used in the adaptation scheme can be designed using basic assumptions on the controlled system. Applicability of control systems in civil engineering is an important topic. It is a critical issue for acceptability of structural control strategies by the industry.

REFERENCES

[1] Burdisso, R. A., "Structural Attenuation due to Seismic Inputs with Active/Adaptive Systems," First World Conference on Structural Control, TA4, 3-12 (1994).

[2] Jansen, L. M., & Dyke, S. J., "Semiactive Control Strategy for MR Dampers: Comparative Study," Journal of Engineering Mechanics 126(8), 795-803 (2000).

[3] Spencer, B. F., Dyke, S. J., Sain, M. K., & Carlson, J. D., "Phenomenological Model for Magnetorheological Dampers," Journal of Engineering Mechanics 123(33), 230-238 (1997).

[4] Dominguez, A., Sedaghati, R., & Stiharu, I., "Semi-Active Vibration Control of Adaptive Structures using Magnetorheological Dampers," AIAA Journal 44(7), 1563-1571 (2006).

[5] Yang, G., "*Large*-Scale Magnetorheological Fluid Damper for Vibration Mitigation: Modeling, Testing and Control," Doctor of Philosophy dissertation, University of Notre Dame, Department of Civil Engineering and Geological Sciences, Notre Dame, Indiana, (2001).

[6] Li, H.-N., & Chang, Z.-G., "Semi-Active Control for Eccentric Structures with MR Damper Based on Hybrid Intelligent Algorithm," Structural Design of Tall and Special Buildings 17(1), 167-280 (2008).

[7] Yang, J. N., Wu, J. C., & Agrawal, A. K., "Sliding Mode Control for Nonlinear and Hysteretic Structures," Journal of Engineering Mechanics 121(12), 1330-1339 (1995).

[8] Wang, S.-G., Yeh, H. Y., & Roschke, P. N., "Robust Control for Structural Systems with Parametric and Unstructured Uncertainties," Proceedings of the American Control Conference, June 25-27, 1109-1114 (2001).

[9] Guo, Y.-Q., & Fei, S.-M., "Simulation Analysis on Intelligent Structures with Magnetorheological Dampers," Journal of Intelligent Material Systems and Structures 19(6), 715-726 (2008).

[10] Shook, D. A., Roschke, P. N., Lin, P.-Y., & Loh, C.-H., "Semi-Active Control for Torsionally-Responsive Structures," Proc. of SPIE - Active and Passive Smart Structures and Integrated Systems 6928, 1-12 (2008).

[11] Suresh, S., Narasimhan, S., & Sundararajan, N., "Adaptive Control of Nonlinear Smart Base-Isolated Buildings using Gaussian Kernel Functions," Structural Control and Health Monitoring 15(4), 585-603 (2008).

[12] Lee, H.-J., Yang, G., Jung, H.-J., Spencer, B. F., & Lee, I.-W., "Semi-Active Neurocontrol of a Base-Isolated Benchmark Structure," Structural Control and Health Monitoring 13, 682-692 (2006).

[13] Lee, H.-J., Jung, H.-J., Cho, S.-W., & Lee, I.-W., "An Experimental Study of Semiactive Modal Neuro-Control Scheme using MR Damper for Building Structure," Journal of Intelligent Metrial Systems and Structures 19(9), 1005-1015 (2008).

[14] Song, X., Ahmadian, M., Southward, S., & Miller, L. R., "An Adaptive Semiactive Control Algorithm for Magnetorheological Suspension Systems," Journal of Vibration and Acoustics 127(5), 493-502 (2005).

[15] Xu, B., Wu, Z., & Yokoyama, K., "Neural Network for Decentralized Control of Cable-Stayed Bridge," Journal of Bridge Engineering 123(3), 229-236 (2003).

[16] Wu, W., Cai, C., & Chen, S., "Experiments on Reduction of Cable Vibration Using MR Dampers," 17th ASCE Engineering Mechanics Conference, 1-8 (2004).

[17] Lord Corporation, www.lord.com, (accessed December 17th, 2008)

[18] Dyke, S., Spencer, B., Sain, M., & Carlson, J., "Modeling and Control of Magnetorheological Dampers for Seismic Response Reduction," Smart Materials and Structures 5(5), 565-575 (1996).

[19] Yoshida, O., Dyke, S. J., Giacosa, L. M., & Truman, K. Z., "Experimental Verification of Torsional Response Control of Asymetric Buildings using MR Dampers," Earthquake Engineering and Structural Dynamics 32(13), 2085-2105 (2003).

[20] Howlett, R. J., & Jain, L. C., [Radial Basis Function Networks 1: Recent Developments in Theory and Applications], Springer-Verlag, (2001).

[21] Sanner, R., & Slotine, J.-J., "Gaussian Networks for Direct Adaptive Control," IEEE Transaction on Neural Networks 3(6), 837-863 (1992).
[22] Kadirkamanathan, V., & Niranjan, M., "A Function Estimation Approach to Sequential Learning with Neural Networks," Neural Computation 5(6), 954-975 (1993).
[23] Norgaard, M., Ravn, O., Poulsen, N. K., & Hansen, L. K., [Neural Networks for Modelling and Control of Dynamic Systems], Springer, (2000).
[24] Freeman, J. A., & Saad, D., "On-Line Learning in Radial Basis Function Networks," Neural Computations 9, 1601-1622 (1997)
[25] Behera, L., Kumar, S., & Patnaik, A., "On Adaptive Learning Rate that Guarantees Convergence in Feedforward Networks," IIEEE Transactions on Neural Networks 17(5), 1116-1125 (2006).
[26] Slotine, J.-J., & Li, W., [Applied Nonlinear Control], Prentice Hall, (1990).
[27] Mizuochi, M., Tsuji, T., & Ohnishi, K, "Multirate Sampling Method for Acceleration Control Systems," IEEE Transactions on Industrial Electronics 54(3), 1629-1634 (2007).
[28] Jiménez, R., & Alvarez-Icaza, L., "A Real-Time Estimation Scheme for Buildings with Intelligent Dissipation Devices, " Mechanical Systems and Signal Processing 21, 2427-2440 (2007).